J Nanostruct Chem (2015) 5:295–303
DOI 10.1007/s40097-015-0161-2

ORIGINAL RESEARCH

Mycogenesis of cerium oxide nanoparticles using *Aspergillus niger* culture filtrate and their applications for antibacterial and larvicidal activities

K. Gopinath[1] · V. Karthika[1] · C. Sundaravadivelan[2] · S. Gowri[1] · A. Arumugam[1]

Received: 5 January 2015 / Accepted: 2 June 2015 / Published online: 22 June 2015

Abstract Cerium oxide nanoparticles (CeO_2 NPs) were synthesized using *Aspergillus niger* culture filtrate. The mycosynthesized CeO_2 NPs were characterized by UV–Visible (UV–Vis), Fourier Transform Infrared (FT-IR), X-ray diffraction (XRD), Micro Raman, Thermogravimetric/Differential Thermal Analysis (TG/DTA), Photoluminescence, and Transmission Electron Microscopy (TEM) analyses. UV–Vis spectrum exhibited a corresponding absorption peak for CeO_2 NPs at 296 nm, and the functional groups present in the fungal filtrate responsible for the synthesis of NPs were analyzed by FT-IR. The further characterization of the mycosynthesized CeO_2 NPs revealed particles of the cubic structure and spherical shape, with the particle sizes ranging from 5 to 20 nm. The antibacterial activity of CeO_2 NPs was examined in respect of two Gram-positive (G+) bacteria (*Streptococcus pneumoniae*, *Bacillus subtilis*) and two Gram-negative (G−) bacteria (*Proteus vulgaris, Escherichia coli*) by disk diffusion method. The test results for CeO_2 NPs at a concentration of 10 mg/mL showed higher activities on the zone of inhibition of up to 10.67 ± 0.33 and 10.33 ± 0.33 mm against *Streptococcus pneumonia* and *Bacillus subtilis*, respectively, The CeO_2 NPs caused 100 % mortality on first instar of *Aedes aegypti* at 0.250 mg/L concentration after 24-h exposure. The mycosynthesis of CeO_2 NPs is a simple, cost-effective and eco-friendly approach and it will also potentially helpful to control pathogenic bacteria and dengue vector.

Keywords *Aspergillus niger* · Culture filtrate · Cerium oxide nanoparticles · Antibacterial activity · Larvicidal activity

Introduction

Nanotechnology has a variety of applications in our daily life. Nanoparticles possess several physical and chemical properties, due to their high surface-to-volume ratio. Cerium oxide (CeO_2) is a semiconductor with a wide band-gap energy (3.19 eV) and a large exciton-binding energy [1], which is used for a wide range of applications such as electronics [2], bio-sensors [3], drug delivery [4], agriculture [5], medical field [6], etc. In general, CeO_2 nanoparticles (CeO_2 NPs) could be synthesized by physical, chemical, and biological (plants and microorganisms) methods [7–15]. Nowadays, biological method offers more advantages such as cost effectiveness, large-scale commercial production, and less time-consuming process [16].

The fungal extracellular membrane containing metabolites, such as enzymes, proteins, and heterocyclic derivatives, can act as quite promising candidates in the production of reducing and capping agents, with good biocatalytic performance [17–20]. Over the last two decades, although many researchers focused on transition metal nanoparticles, very few works have been conducted toward the synthesis of metal oxide nanoparticles. In this respect, CeO_2 NPs were synthesized using *Humicola* sp. culture

✉ A. Arumugam
sixmuga@yahoo.com

[1] Department of Nanoscience and Technology, Alagappa University, Karaikudi 630 004, Tamil Nadu, India

[2] Department of Zoology, Vivekanandha College of Arts and Sciences for Women, Elayampalayam 637 205, Tamil Nadu, India

filtrate [21]. Moreover, the synthesized nanoparticles are highly stable, water dispersible and exhibit high fluorescent properties and also lack agglomeration, as they are capped naturally by the enzymes secreted from the fungus [21–23].

Aspergillus niger is a filamentous ascomycete fungus and group of saprophytic molds. Generally, *A. niger* can reproduce by means of conidia. It can grow at 6–47 °C and pH 1.4–9.8. It is an important industrial fungus used for producing citric acid, amylases, lipases, cellulases, xylanases, proteases production, and for removal of heavy metal ions from waste waters [24, 25]. Previously, metal nanoparticles were synthesized using *A. niger* culture filtrate. Fungal filtrate contains enzymes, and anthraquinone compounds are more responsible for reducing and capping processes. The synthesized metal nanoparticles showed better antibacterial and larvicidal activities against bacterial pathogens and mosquito vectors [17, 26].

In the present investigation, we propose the synthesis and the characterization of CeO_2 NPs using *A. niger* culture filtrate and their potential applications for antibacterial and larvicidal activities. The report on the mycosynthesis of CeO_2 NPs describes it as a simple, rapid, water miscible, nontoxic and it provides high yield on a large scale. It can also be used as an alternative biocontrol agent in near future.

Materials and methods

Identification of fungus

Aspergillus niger culture (Fig. 1a) was collected from the PG and the Research Department of Plant Biology and Plant Biotechnology, Ramakrishna Mission Vivekananda College, Chennai. The Identified fungus *A. niger* have small size conidia (Fig. 1b) observed by light microscope (Euromex GE3045, Netherlands) at a magnification of 40X.

Mycosynthesis of cerium oxide nanoparticles

Fungus, *A. niger* was inoculated in Czapek-Dox-Broth (CDB) medium, and the flask was incubated at 37 °C, at 120 rpm for 72 h. After the incubation, the produced fungal spores with small white ball-like structure were observed in the medium (Fig. 1c). The fungal culture medium was filtered using Whatman No.1 filter paper, and the collected fungal filtrate was stored at 4 °C for further use. Thereafter, 3.72 g of $CeCl_3{\cdot}7H_2O$ was added to 100 mL of fungal filtrate. This solution was stirred constantly at 80 °C for 4–6 h. A white precipitate was formed, and then it became a yellowish brown in color upon continuous stirring in the flask. Further, the precipitate was calcined at 350 and 400 °C for 2 h. Finally, CeO_2 NPs in the form of nanopowders were obtained.

Characterization

The mycosynthesized CeO_2 NPs were characterized by UV–Vis spectroscopy (Shimadzu, UV-1800) in the wavelengths ranging from 200 to 800 nm continuously operating at a resolution of 1 nm, and FT-IR analysis was carried out in the frequency range of 400–4000 cm^{-1}. The XRD pattern was recorded using Cu Kα radiation ($\lambda = 1.54060$ Å) with nickel monochromator with 2θ ranging from 10^o to 80^o. The Micro Raman analysis was carried out using 0.5 Focal length triple grating monochromotor excitation source with Ar^+ laser at 514.5-nm wavelength (Princeton Acton SP2500, CS spectrometer). Thermal behavior of the mycosynthesized CeO_2 NPs was studied by TG/DTA analysis under nitrogen atmosphere (Seiko SSC 5200H), and Photoluminescence measurement was carried out on a luminescence spectrophotometer (Perkin Elmer LS-5513, USA) using xenon lamp as the excitation source at room temperature. The morphology of the CeO_2 NPs was examined using TEM. Samples for TEM analysis were

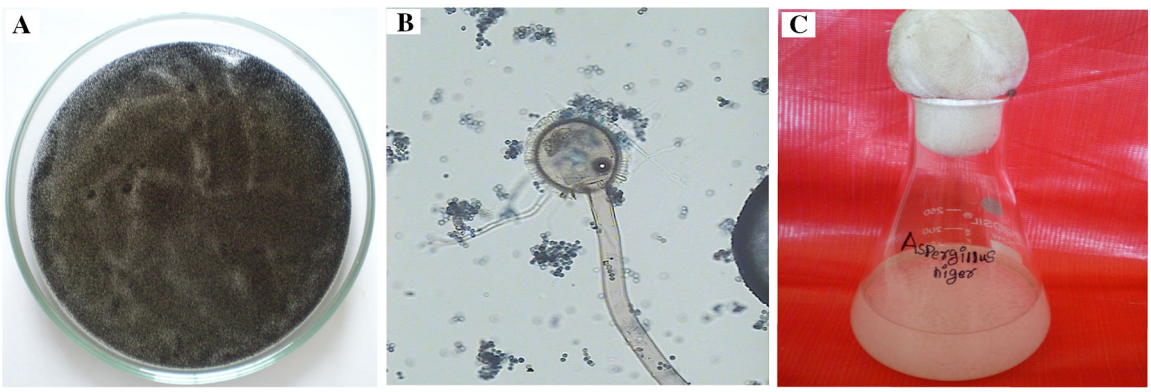

Fig. 1 **a** *Aspergillus niger* culture plate, **b** *A. niger* conidia, **c** Fungal culture in Czapek-Dox-Broth medium

prepared by drop coating the nanoparticle solutions on carbon-coated copper grids at room temperature. The excess nanoparticle's solution was removed using filter paper. The copper grid was finally dried at room temperature and was subjected to TEM analysis (Tecnai F20) operated at an accelerating voltage of 200 kV.

Antibacterial activity

The antibacterial activity of the mycosynthesized CeO_2 NPs was examined against two Gram-positive (G+) (*Streptococcus pneumoniae*, *Bacillus subtilis*) and Gram-negative (G−), (*Proteus vulgaris, Escherichia coli*) pathogenic bacteria using disk diffusion method [27]. The bacterial strains were grown in nutrient broth at 37 °C until the bacterial suspension reached 1.5×10^8 CFU/mL. Approximately 20 mL of molten nutrient agar was poured into the Petri dishes and cooled. All the bacterial suspension was swapped over the medium, the disks were loaded at three different concentrations 1, 5, and 10 mg/mL of CeO_2 NPs using sterile distilled water, and then they were placed over the medium using sterile forceps. The plates were then incubated at 37 °C for 24 h. The inhibition zone formed around each disk was measured, and each experiment was conducted in triplicate.

Larvicidal and pupicidal activities

The larvicidal and pupicidal activities of CeO_2 NPs were evaluated, following the method of the World Health Organization (WHO) [28] with slight modifications. A bioefficacy test was conducted against developmental stages: I–IV instar and pupa of *A. aegypti*. Different test concentrations (0.010, 0.050, 0.100, 0.200, and 0.250 mg/L) of CeO_2 NPs and *A. niger* fungal culture filtrates were prepared in 200 mL deionized water in autoclaved glass bottles of 250-mL capacity. To find the larvicidal and pupicidal activities of CeO_2 NPs and fungal culture filtrate alone, early stages of 20 larvae (I–IV) and pupa were exposed in each test to different concentrations. Similarly, each test included a set of control group (distilled water), and the mortality rate was recorded after 24-h exposure period. Each test was conducted with five replicates.

Statistical analysis

The percent mortality was observed, and the average mortality data were subjected to Probit analysis for calculating LC_{50} and, lower and upper confidence limit values at 95 % using the SPSS software package 9.0 ver. Results with p value of <0.05 were considered to be statistically significant.

Results and discussion

UV–Visible spectroscopy

Mycosynthesized CeO_2 NPs were subjected to the UV–Vis spectrum analysis in the range from 200 to 800 nm continuously. It exhibited a well-defined absorption peak at 296 nm which indicates that the synthesized CeO_2 NPs have a better optical property (Fig. 2). The observed peak at 296 nm corresponds to the fluorite cubic structure of CeO_2 NPs due to the quantum size effect of the blue shift in UV–Vis spectrum and confirms the charge between the O 2*p* and Ce 4*f* states in O^{2-} and Ce^{4+} [3, 14]. The observed result is consistent with the previous report [29].

Fourier-transform infrared spectroscopy

FT-IR analyses of the fungal culture filtrate, the as-synthesized sample, the calcined samples at 350 and 400 °C were observed (Fig. 3). FT-IR spectra showed the potential biomolecules responsible for the reduction of $CeCl_3$ ions for the synthesis of CeO_2 NPs while reacting with *A. niger* culture filtrate. The group of strong, intense bands was observed at 3425, 2360, and 1340 cm^{-1}. The intense band at 3425 cm^{-1} corresponds to (O–H) mode of hydroxyl molecules. The bands observed at 2360 and 1340 cm^{-1} correspond to CeO_2 NPs. These CO_2 bands may arise due to some trapped CO_2 in air ambience. The band at 1642 cm^{-1} corresponds to the bending of H–O–H which is partly overlapping the O–C–O stretching band [30]. In our case, Ce–O stretching is observed at 468 cm^{-1}. The FT-IR spectra for the 400 °C calcined samples showed a band at 3425 cm^{-1} of (OH) hydroxyl molecules transmittance percent, which was reduced compared to the spectra of

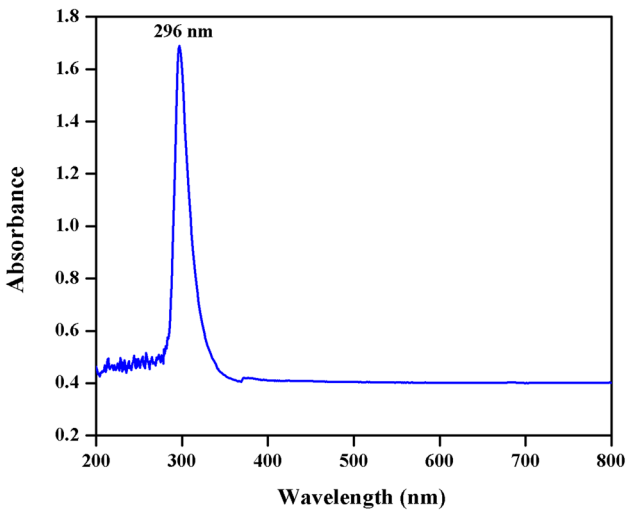

Fig. 2 UV–Visible spectrum of the mycosynthesized CeO_2 NPs

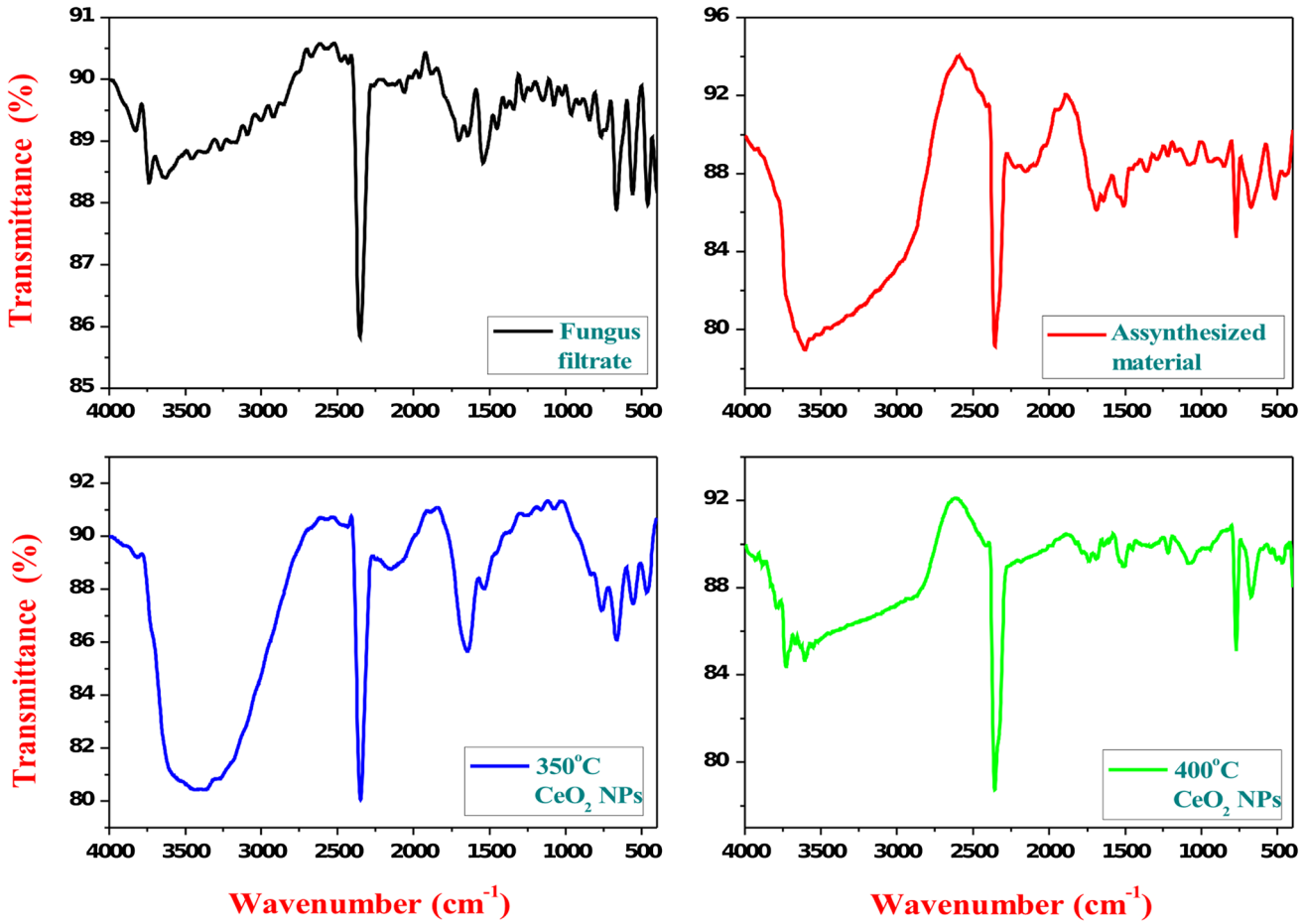

Fig. 3 FTIR-spectra of fungal culture filtrate, as-synthesized sample, and calcined samples at 350 and 400 °C

350 °C calcined samples which is due to the formation of the high crystalline nature of CeO_2 NPs [3, 30].

X-ray diffraction and Micro Raman spectroscopy

X-ray diffraction patterns were recorded for the as-synthesized and calcined CeO_2 NPs. The as-synthesized and 350 °C calcined samples have not shown any clear, intense peaks, which is due to the amorphous state (Fig. 4). In addition, the calcined sample at 400 °C exhibited XRD peaks at 28.49°, 33.01°, 47.42°, and 56.28° which can be indexed with (111), (200), (220), and (311) planes, respectively, for the cubic fluorite structure of CeO_2 NPs in the standard data (JCPDS card no: 89-8436). It clearly showed that the peaks become sharper and narrower with the increasing temperature. The low intense peaks at 59.01°, 69.34°, 76.66°, and 79.17° belonged to (222), (400), (331), and (420) planes, respectively [21, 31]. The extra unassigned peaks at 31.51° and 45.25° were observed

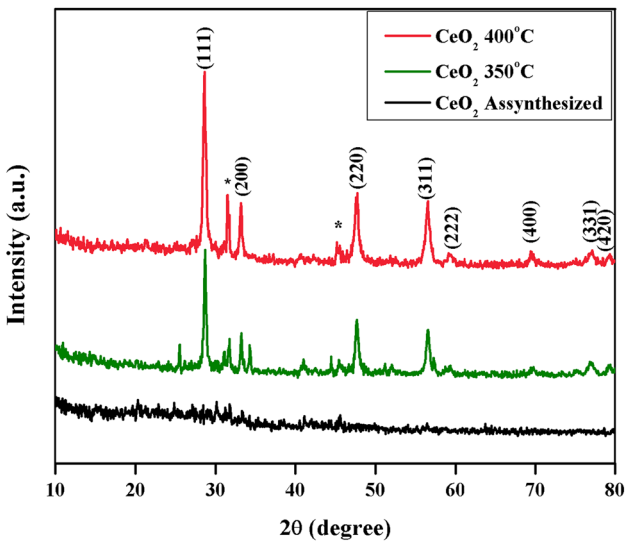

Fig. 4 X-ray diffraction patterns of mycosynthesized CeO_2 NPs (*asterisk* shows unassigned peaks)

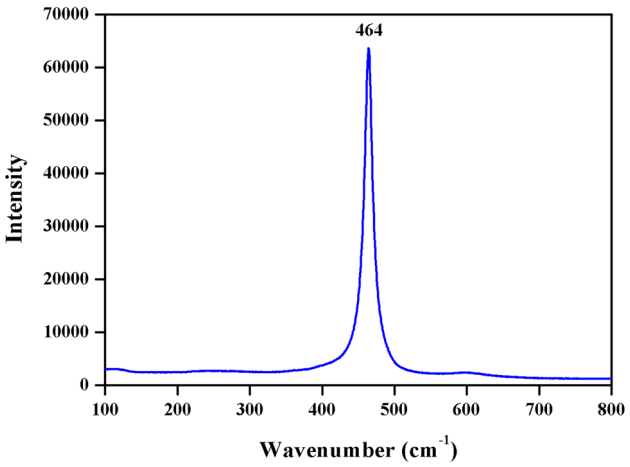

Fig. 5 Raman spectrum of the mycosynthesized CeO_2 NPs calcined at 400 °C

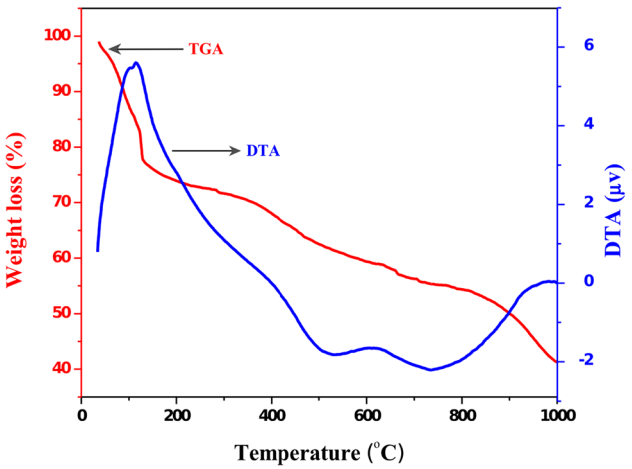

Fig. 6 TGA/DTA curves of as-synthesized CeO_2 nanopowders

in the XRD analysis of CeO_2 NPs, which is due to the sulfur oxide impurities [21]. The average crystalline size was estimated using the Scherrer formula, and it is estimated to be around 14.95 nm [20]. The mycosynthesized CeO_2 NPs was further elucidated by Micro Raman spectroscopy, and it exhibited a strong, intense band at 464 cm^{-1} (Fig. 5). The Raman active mode is attributed to a symmetrical stretching of Ce 8O, which generally corresponds to F_{2g} Raman active mode of fluorite cubic structure [15, 32].

TG/DTA analysis

Thermogravimetric/differential thermal analysis measurement was performed to examine the thermal stability of the crystalline sample. The TG/DTA curves for the as-synthesized sample recorded in the temperature range from 35 to 1000 °C at a heating rate of 20 °C/min are shown in Fig. 6. The TGA curves exhibited three stages of decomposition. The first minor weight loss step (9.84 %) from 35 to 100 °C, the second (13.49 %) from 100 to 150 °C, the third (15.25 %) from 150 to 540 °C and also a dramatic weight loss step (15.25 %) were observed from 540 to 1000 °C. The minor weight loss from 35 to 150 °C was related to the losses of water, moisture, and extracellular fungal components. The slight weight losses of fungal organic components were observed with chlorine. Almost no weight loss could be observed above 600 °C [14, 30, 31]. The two exothermic peaks observed at 115 and 615 °C on the DTA curve represent the strong and minor peaks, respectively, which confirms the combustion of organic residues (115 °C), and decomposition of some residual, absorbed species and oxygen loss at higher temperature (615 °C) [31]. Above 740 °C, the gradual increase in DTA curve was ascribed to the phase change or valence variation of cerium [3].

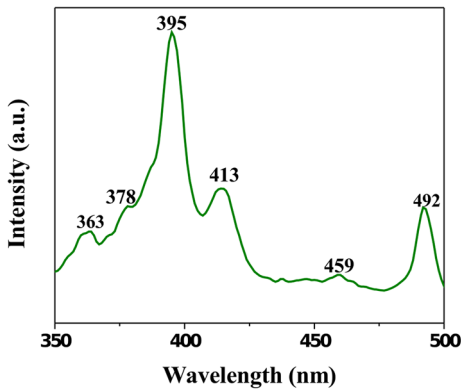

Fig. 7 Photoluminescence spectrum of mycosynthesized CeO_2 NPs calcined at 400 °C

Photoluminescence spectroscopy

The room temperature PL spectrum of the CeO_2 NPs measured using Xenon laser of 290 nm (Fig. 7). The spectrum of the CeO_2 NP sample mainly consists of six emission peaks; weak blue bands at 363, 378, 413, and 459 nm; a broad emission band at 395 nm; and a weak blue–green band at 492 nm. The dependence of PL blue-shift peak on CeO_2 NPs concentration has also been observed. This phenomenon has been explained by the charge transition from the *4f* band to the valance band of the CeO_2 NPs. In this sample, the weak blue and weak blue–green emissions are possibly due to surface defects in the CeO_2 NPs, and the low intensity of the green emission peak due to the low density of oxygen vacancies during the preparation of sample. Broad peaks centered at 395 nm for

the CeO_2 sample calcined at 400 °C originate from the defect states existing between the Ce 4*f* state and O 2*p* valence band. The room temperature emission intensity for the CeO_2 sample calcined at 400 °C was attributed to its better crystallinity [15].

Transmission electron microscopy

The morphology and the structure of the CeO_2 NPs were observed under TEM (Fig. 8a, b). The images with corresponding selected-area electron diffraction (SAED) patterns and high-resolution TEM images of the CeO_2 NPs were recorded. The mycosynthesized CeO_2 NPs exhibit cubic and spherical morphologies with their sizes ranging from 5 to 20 nm with an average size of about 10 nm. The SAED patterns of CeO_2 NPs show the characteristic ring pattern of fluorite cubic structure, and they confirm the higher degree of crystallinity of CeO_2 NPs (Fig. 8c) [30].

Antibacterial activity

The antibacterial activity of CeO_2 NPs was performed against two Gram-positive and Gram-negative bacterial human pathogens using three different concentrations of 1, 5, and 10 mg/mL of CeO_2 NPs (Fig. 9). The CeO_2 NPs of 1 mg/mL concentration did not show any inhibitory effect of zone formation in all tested strains. Then, CeO_2 NPs of 5 mg/mL concentration showed a modulated effect of inhibition zones at *Proteus vulgaris* in 3.67 ± 0.33 mm, *Escherichia coli* in 3.33 ± 0.33 mm, *Streptococcus pneumonia* in 3.33 ± 0.33 mm, and *Bacillus subtilis* in 4.67 ± 0.33 mm. The inhibition zones with significant effect shown by the CeO_2 NPs of 10 mg/mL concentration of are *Streptococcus pneumonia* in 10.67 ± 0.33 mm, *Bacillus subtilis* in 10.33 ± 0.33 mm, *Proteus vulgaris* in 8.33 ± 0.33 mm, and *Escherichia coli* in 6.33 ± 0.33 mm (Fig. 10). However, the CeO_2 NPs of 10 mg/mL concentration showed higher impact of antibacterial activity in Gram-positive bacteria compared to Gram-negative bacteria. This is because the Gram-positive bacterial cell wall contains a thick layer of peptidoglycan, which is attached to teichoic acids, and this may be the reason for the interaction with CeO_2 NPs in antibacterial activity. The zone of inhibition effect of antibacterial activity depends upon the concentration of CeO_2 NPs. The observed results could be attributed to a binding of metal and metal oxide nanoparticles on to the bacterial cell wall due to the electrostatic attraction between the negatively charged bacteria and the positively charged nanoparticles. This interaction not only inhibits the bacterial growth, but it also induces the generation of the reactive oxygen species (ROS), which leads to cell death [33]. The actual mechanism of antibacterial activity of CeO_2 NPs could be an interference with the bacteria cell membrane and binding with mesosome, which thus disturbs the mesosomal functions of cellular respiration, DNA replication, cell division, and increases the surface area of bacterial cell membrane; these intracellular functional changes of oxidative stress are induced by ROS generation due to cell death. The results observed forthe CeO_2 NPs of 10 mg/mL concentration showed the most significant effect of antibacterial activity against the tested Gram-positive and -negative bacteria due to the strong electrostatic forces required to bind the bacterial cell membrane to cause the inhibition of bacterial growth. On the contrary, CeO_2 NPs did not show any antibacterial activity in previous reports, at 10 μg and 10 mg concentrations [29, 34].

Larvicidal and pupicidal activities

Larvicidal and pupicidal activities of CeO_2 NPs and *A. niger* fungus filtrate were observed against I–IV instar and pupa of *A. aegypti* at five different concentrations (Table 1). The high mortality rates ranked in descending order against first (100 %), second (92 %), third (76 %),

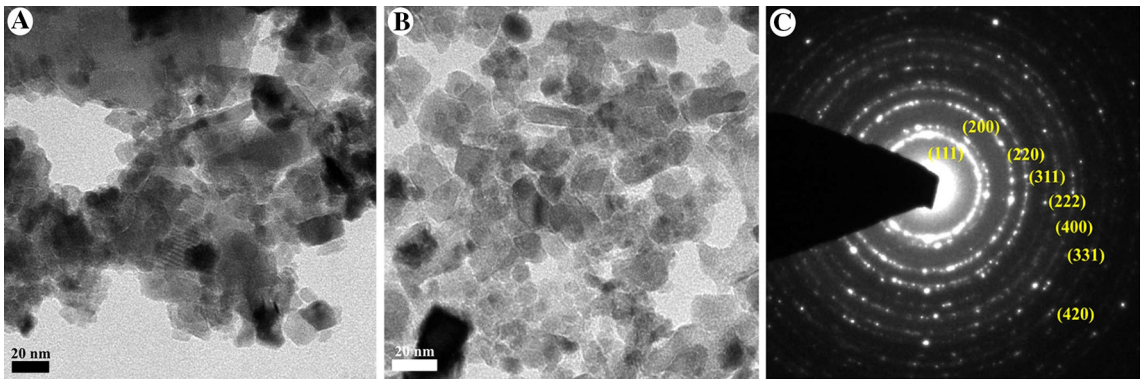

Fig. 8 **a**, **b** TEM images of mycosynthesized CeO_2 NPs calcined at 400 °C, c selected-area electron diffraction of CeO_2 NPs

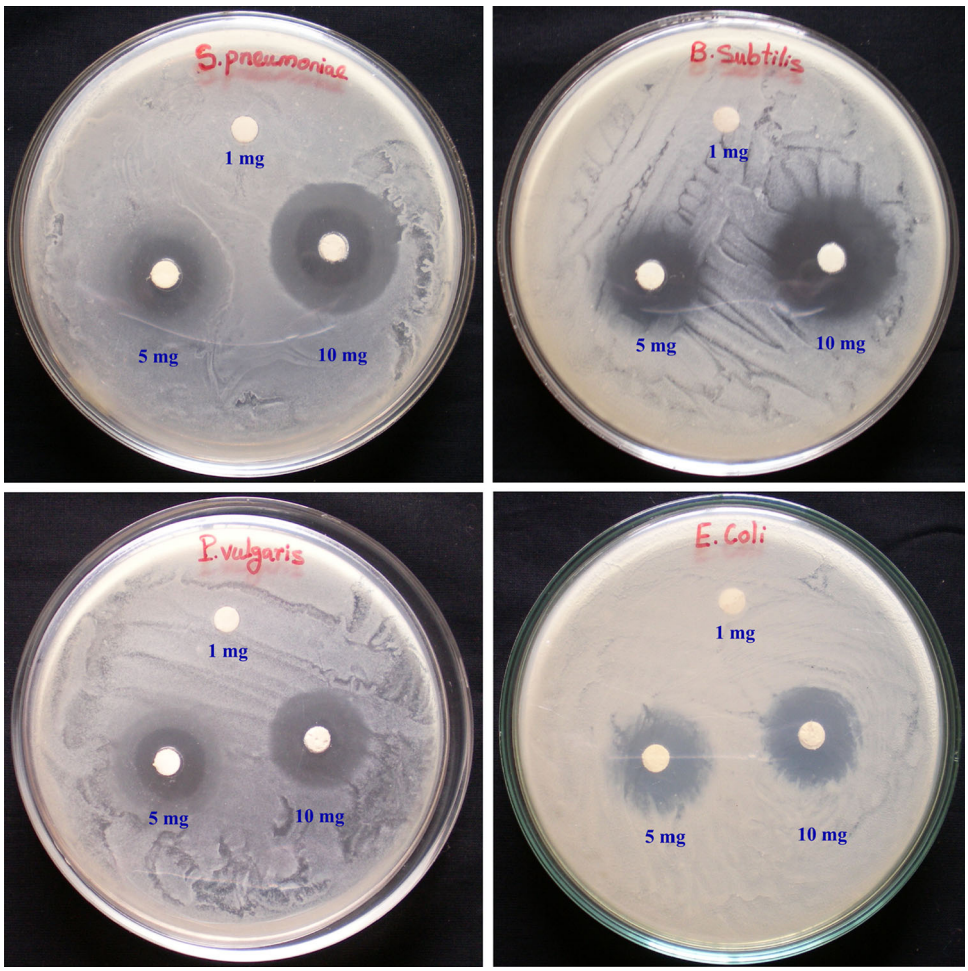

Fig.9 Zones of inhibition in CeO_2 NPs at different concentrations against Gram-positive and Gram-negative bacteria

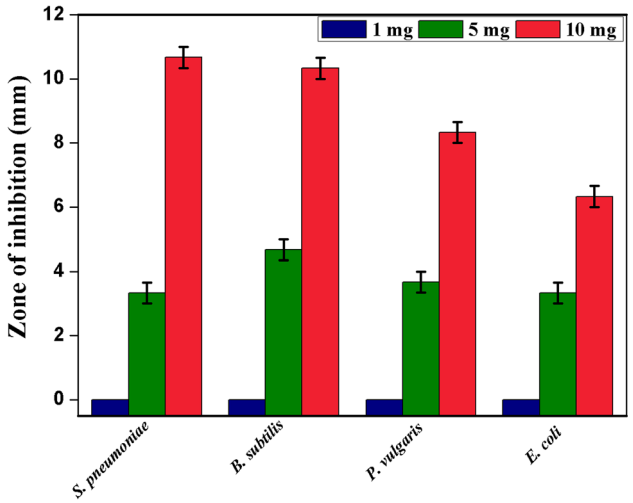

Fig. 10 Antibacterial activities of CeO_2 NPs against Gram-positive and Gram-negative bacteria

fourth (70 %), and pupa (70 %) were observed at 0.250 mg/L concentration after 24-h exposure period, and their LC_{50} values were 0.033, 0.045, 0.074, 0.085, and 0.116 %, respectively. The *A. niger* fungus filtrate showed very low mortality rates of 46, 40, 32, and 28 for I–IV instar and 20 % for pupa, respectively, after 24-h exposure period, and their LC_{50} values were calculated as 0.297, 0.353, 0.426, and 0.453, and 0.467 %, respectively, and no mortality was observed in control. Similar kinds of mortality were observed when exposed to Ag NPs produced from *Cochliobolus lunatu* [35], and interestingly, 100 % mortality was recorded in early second instar after 1-h exposure of Ag NPs synthesized using *Chrysosporium tropicum* [17]. The CeO_2 NPs **showed 2–3-fold higher mortality rate compared to *A. niger* fungus filtrate treatment alone. The exact mechanism is not known clearly till now, even though the obtained results suggest that the CeO_2 NPs could be interrupting the membrane permeability and thus leading to cell death. Recently, it was reported that the penetration of NPs when treated with laveral membrane results in the death of larvae due to interaction with cell molecules [28]. In addition, once NPs reach their midgut epithelial membrane, the enzymes become inactivated, and generate peroxide leading to cell death [36, 37].

Table 1 Anti-developmental activity of CeO_2 NPs produced using *A. niger* extract against *A. aegypti*

Test substance	Instar stages	Percent mortality (%) ± SE					LC_{50}	95 % Confidence Limit		χ^2 ($df = 3$)#
		0.010 mg/L	0.050 mg/L	0.100 mg/L	0.200 mg/L	0.250 mg/L		LCL	UCL	
A. niger extract	I	12 ± 1.294	18 ± 0.946	22 ± 1.294	30 ± 1.189	46 ± 1.337	0.297	0.248	0.389	1.831
	II	10 ± 0.000	18 ± 1.294	20 ± 1.189	24 ± 1.337	40 ± 0.000	0.353	0.284	0.506	3.482
	III	10 ± 1.189	12 ± 1.480	16 ± 2.093	20 ± 1.189	32 ± 1.615	0.426	0.329	0.682	1.320
	IV	8 ± 0.946	10 ± 1.189	14 ± 1.047	18 ± 1.189	28 ± 2.317	0.453	0.347	0.742	0.859
	Pupae	2 ± 0.946	6 ± 1.337	12 ± 0.946	14 ± 2.502	20 ± 1.189	0.467	0.363	0.738	3.311
CeO_2 NPs	I	46 ± 1.337	52 ± 1.813	72 ± 1.961	88 ± 1.615	100 ± 0.000	0.033	0.041	0.071	7.016
	II	42 ± 1.615	48 ± 1.615	68 ± 1.615	80 ± 1.778	92 ± 0.946	0.045	0.017	0.065	2.605
	III	38 ± 2.082	42 ± 0.946	60 ± 0.000	72 ± 0.946	76 ± 1.047	0.074	0.412	0.100	2.102
	IV	38 ± 0.946	42 ± 0.946	56 ± 1.742	70 ± 1.414	70 ± 0.000	0.085	0.047	0.114	1.929
	Pupae	32 ± 1.480	38 ± 1.480	52 ± 0.946	62 ± 0.946	70 ± 0.000	0.116	0.086	0.145	1.111

LC_{50} lethal concentration 50, *LCL* lower confidence limit, *UCL* upper confidence limit, χ^2 Chi square value, *df* degrees of freedom

* Values are mean of five replicates with ± SE

\# Significant at $p < 0.05$ level

Conclusion

CeO_2 NPs have been successfully synthesized using *A. niger* culture filtrate. The detailed characterization study revealed the formation of CeO_2 NPs cubic fluorite structure and a spherical morphology with the average size of 5 nm. Mycosynthesized CeO_2 NPs showed their potent antibacterial and larvicidal activities against pathogenic bacteria and dengue vector. The mycosynthesis of CeO_2 NPs is a simple, reliable, cost effective and eco-friendly approach, and it can also be extended to synthesize other metal oxide NPs.

Acknowledgments The authors gratefully thank the School of Physics, Alagappa University, Karaikudi, for extending the XRD facility.

Conflict of interest The Author(s) declare that they have no conflict of interest.

Authors' contributions KG, VK, CS, and SG completed the nanoparticles synthesis, characterization, and applications. AA carried out the manuscript preparation. All authors read and approved the final manuscript.

References

1. Miao, J.J., Wang, H., Li, Y.R., Zhu, J.M., Zhu, J.J.: Ultrasonic-induced synthesis of CeO_2 nanotubes. J. Cryst. Growth **281**, 525–529 (2005)
2. Thakur, S., Patil, P.: Rapid synthesis of cerium oxide nanoparticles with superior humidity-sensing performance. Sens. Actuator B **194**, 260–268 (2014)
3. Khan, S.B., Faisal, M., Rahman, M.M., Jamal, A.: Exploration of CeO_2 nanoparticles as a chemi-sensor and photo-catalyst for environmental applications. Sci. Total Environ. **409**, 2987–2992 (2011)
4. Patil, S., Sandberg, A., Heckert, E., Self, W., Seal, S.: Protein adsorption and cellular uptake of cerium oxide nanoparticles as a function of zeta potential. Biomaterials **28**, 4600–4607 (2007)
5. Zhang, P., Ma, Y., Zhang, Z., He, X., Zhang, J., Guo, Z., Tai, R., Zhao, Y., Chai, Z.: Biotransformation of ceria nanoparticles in cucumber plants. ACS Nano **11**, 9943–9950 (2012)
6. Thill, A., Zeyons, O., Spalla, O., Chauvat, F., Rose, J., Auffan, M., Flank, A.M.: Cytotoxicity of CeO_2 nanoparticles for *Escherichia coli*. Physico-chemical insight of the cyttoxicity mechanism. Environ. Sci. Technol. **40**, 6151–6156 (2006)
7. Panahi-Kalamuei, M., Alizadeh, S., Mousavi-Kamazani, M., Salavati-Niasari, M.: Synthesis and characterization of CeO_2 nanoparticles via hydrothermal route. J. Ind. Eng. Chem. **21**, 1301–1305 (2015)
8. Hu, J., Li, Y., Zhou, X., Cai, M.: Preparation and characterization of ceria nanoparticles using crystalline hydrate cerium propionate as a precursor. Mater. Lett. **61**, 4989–4992 (2007)
9. Wang, H., Zhu, J.J., Zhu, J.M., Liao, X.H., Xu, S., Ding, T., Chen, H.Y.: Preparation of nanocrystalline ceria particles by sonochemical and microwave assisted heating methods. Phys. Chem. **4**, 3794–3799 (2002)
10. Soren, S., Bessoi, M., Parhi, P.: A rapid microwave initiated polyol synthesis of cerium oxide nanoparticles using different cerium precursors. Ceram. Int. **41**, 8114–8118 (2015)
11. Darroudi, M., Hakimi, M., Sarani, M., Kazemi Oskuee, R., Khorsand Zak, A., Gholami, L.: Facile synthesis, characterization, and evaluation of neurotoxicity effect of cerium oxide nanoparticles. Ceram. Int. **39**, 6917–6921 (2013)
12. Yao, S.Y., Xie, Z.H.: Deagglomeration treatment in the synthesis of doped-ceria nanoparticles via coprecipitation route. J. Mater. Process. Technol. **186**, 54–59 (2007)
13. Darroudi, M., Hoseini, S.J., Oskuee, R.K., Hosseini, H.A., Gholami, L., Gerayli, S.: Food-directed synthesis of cerium oxide nanoparticles and their neurotoxicity effects. Ceram. Int. **40**, 7425–7430 (2014)

14. Maensiri, S., Masingboon, C., Laokul, P., Jareonboon, W., Promarak, V., Anderson, P.L., Seraphin, S.: Egg white synthesis and photoluminescence of platelike clusters of CeO_2 nanoparticles. Cryst. Growth Des. **7**, 950–955 (2007)
15. Maensiri, S., Labuayai, S., Laokul, P., Klinkaewnarong, J., Swatsitang, E.: Structure and optical properties of CeO_2 nanoparticles prepared by using lemongrass plant extract solution. Jpn. J. Appl. Phys. **53**, 06–14 (2014)
16. Mohanpuria, P., Rana, N.K., Yaday, S.K.: Biosynthesis of nanoparticles technological concepts and future applications. J. Nanopart. Res. **10**, 507–517 (2008)
17. Soni, N., Prakash, S.: Efficacy of fungus mediated silver and gold nanoparticles against *Aedes aegypti* larvae. J. Rep. Parasitol. **110**, 175–184 (2012)
18. Balaji, D.S., Basavaraja, S., Deshpande, R., Bedre Mahesh, D., Prabhakar, B.K., Venkataraman, A.: Extracellular biosynthesis of functionalized silver nanoparticles by strains of *Cladosporium cladosporioides*. Colloids Surf. B **68**, 88–92 (2009)
19. Rajakumar, G., Abdul Rahuman, A., Mohana Roopan, S., Gopiesh Khanna, V., Elango, G., Kamaraj, C., Abduz Zahir, A., Velayutham, K.: Fungus-mediated biosynthesis and characterization of TiO_2 nanoparticles and their activity against pathogenic bacteria. Spectrochim. Acta A **91**, 23–29 (2012)
20. Gopinath, K., Arumugam, A.: Extracellular mycosynthesis of gold nanoparticles using *Fusarium solani*. Appl. Nanosci. **4**, 657–662 (2014)
21. Khana, S.A., Ahamad, A.: Fungus mediated synthesis of biomedically important cerium oxide nanoparticles. Mater. Res. Bull. **48**, 4134–4138 (2013)
22. Bhainsa, K.C., D'Souza, S.F.: Extracellular biosynthesis of silver nanoparticles using the fungus *Aspergillus fumigates*. Colloids Surf. B **47**, 160–164 (2006)
23. Gopal, J.V., Thenmozhi, M., Kannabiran, K., Rajakumar, G., Velayutham, K., Abdul Rahuman, A.: Actinobacteria mediated synthesis of gold nanoparticles using *Streptomyces* sp. VITDDK3 and its antifungal activity. Mater. Lett. **93**, 360–362 (2013)
24. Pandey, A., Selvakumar, P., Soccol, C.R., Nigam, P.: Solid state fermentation for the production of industrial enzymes. Curr. Sci. India **77**, 149–162 (1999)
25. Kapoora, A., Viraraghavana, T., Cullimoreb, D.R.: Removal of heavy metals using the fungus *Aspergillus niger*. Bioresour Technol. **70**, 95–104 (1999)
26. Gade, A.K., Bonde, P.P., Ingle, A.P., Marcato, P.D., Duran, N., Rai, M.K.: Exploitation of *Aspergillus niger* for synthesis of silver nanoparticles. J. Biobased Mater. Bioenergy **2**, 243–247 (2008)
27. Gopinath, K., Karthika, V., Gowri, S., Arumugam, A.: Antibacterial activity of ruthenium nanoparticles synthesized using *Gloriosa superba* L. leaf extract. J. Nanostruct. Chem. **4**, 83 (2014)
28. Sundaravadivelan, C.: Nalini Padmanabhan, M., Sivaprasath, P., Kishmu, L.: Biosynthesized silver nanoparticles from *Pedilanthus thithymaloides* leaf extract with anti-developmental activity against larval instars of *Aedes aegypti* L. (Diptera; Culicidae). Parasitol. Res. **112**, 303–311 (2013)
29. Arumugam, A., Karthikeyan, C., Haja Hameed, A.S., Gopinath, K., Gowri, S., Karthika, V.: Synthesis of cerium oxide nanoparticles using *Gloriosa superba* L. leaf extract and their structural, optical and antibacterical properties. Mater. Sci. Eng. C **49**, 408–415 (2015)
30. Phoka, S., Laokul, P., Swatsitang, E., Promarak, V., Seraphin, S., Maensiri, S.: Synthesis, structural and optical properties of CeO_2 nanoparticles synthesized by a simple polyvinyl pyrrolidone (PVP) solution route. Mater. Chem. Phys. **115**, 423–428 (2009)
31. Suresh, R., Ponnuswamy, V., Mariappan, R.: Effect of annealing temperature on the microstructural, optical and electrical properties of CeO_2 nanoparticles by chemical precipitation method. Appl. Surf. Sci. **273**, 457–464 (2013)
32. Krishnan, A., Sreeremya, T.S., Murray, E., Ghosh, S.: One-pot synthesis of ultra-small cerium oxide nanodots exhibiting multicoloured fluorescence. J. Colloid Interf. Sci. **389**, 16–22 (2013)
33. Gopinath, K., Gowri, S., Arumugam, A.: phytosynthesis of silver nanoparticles using *Pterocarpus santalinus* leaf extract and their antibacterial properties. J. Nanostruct. Chem. **3**, 68 (2013)
34. Ravikumar, S., Gokulakrishnan, R., Boomi, R.: In vitro antibacterial activity of the metal oxide nanoparticles against urinary tract infectious bacterial pathogens. Asian Pac. J. Trop. Dis. **2**, 85–89 (2012)
35. Salunkhe, R.B., Patil, S.V., Patil, C.D., Salunke, B.K.: Larvicidal potential of silver nanoparticles synthesized using fungus *Cochliobolus lunatus* against *Aedes aegypti* (Linnaeus, 1762) and *Anopheles stephensi* Liston (Diptera: Culicidae). Parasitol. Res. **109**, 823–831 (2011)
36. Raffi, M., Hussain, F., Bhatti, T.M., Akhter, J.I., Hameed, A., Hasan, M.M.: Antibacterial characterization of silver nanoparticles against *E. coil* ATCC-15224. J. Mater. Sci. Technol. **24**, 192–196 (2008)
37. Rawani, A., Ghosh, A., Chandra, G.: Mosquito larvicidal and antimicrobial activity of synthesized nanocrystalline silver particles using leaves and green berry extract of *Solanum nigrum* L. (Solanaceae: Solanales). Acta Trop. **128**, 613–622 (2013)